

Wet-environment Evapotranspiration and Precipitation Standardized Index (WEPSI) for drought assessment and monitoring

Ali Khoshnazar^{1,1}, Gerald Augusto Corzo Perez^{1,1}, Vitali Diaz^{2,2}, and Milad Aminzadeh^{3,3}

¹IHE Delft Institute for Water Education

²Delft University of Technology

³Isfahan University of Technology

November 30, 2022

Abstract

Drought is a major threat to global agriculture and can trigger or intensify food price increase and migration. Assessment and monitoring are essential for proper drought management. Drought indices play a fundamental task in this respect. This research introduces the Wet-environment Evapotranspiration and Precipitation Standardized Index (WEPSI) for drought assessment and monitoring. WEPSI is inspired by the Standardized Precipitation Evapotranspiration Index (SPEI), in which water supply and demand are incorporated into the drought index calculation. WEPSI considers precipitation (P) for water supply and wet-environment evapotranspiration (ET_w) for water demand. We use an asymmetric complementary relationship to calculate ET_w using actual (ET_a) and potential evapotranspiration (ET_p). WEPSI is tested in the transboundary Lempa River basin located in the Central American dry corridor. ET_w is estimated based on evapotranspiration data calculated using the Water Evaluation And Planning (WEAP) system hydrological model. To investigate the performance of our introduced drought index, we compare it with two well-known meteorological indices (Standardized Precipitation Index and SPEI), together with a hydrological index (Standardized Runoff Index), in terms of correlation and mutual information (MI). We also compare drought calculated with WEPSI and historical information, including crop cereal production and Oceanic Niño Index (ONI) data. The results show that WEPSI has the highest correlation and MI compared with the three other indices used. It is also consistent with the records of crop cereal production and ONI. These findings show that WEPSI can be applied for agricultural drought assessments.

Wet-environment Evapotranspiration and Precipitation Standardized Index (WEPSI) for drought assessment and monitoring

A. Khoshnazar¹, G. A. Corzo Perez¹, V. Diaz^{1,2}, and M. Aminzadeh³

¹IHE Delft Institute for Water Education, The Netherlands;

²Water Resources Section, Delft University of Technology, The Netherlands;

³Department of Civil Engineering, Isfahan University of Technology, Iran;

Corresponding author: Ali Khoshnazar (ali.khoshnazaar@gmail.com; a.khoshnazar@un-ihe.org), Gerald A. Corzo Perez (g.corzo@un-ihe.org), Vitali Diaz (v.diazmercado@tudelft.nl; vitalidime@gmail.com)

Key Points:

- We introduce the Wet-environment Evapotranspiration and Precipitation Standardized Index (WEPSI)
- WEPSI highly correlates with the well-known hydrological drought index SRI
- Droughts calculated with WEPSI coincide with the declines in crop cereal production in the region

Keywords: WEPSI; drought index; drought assessment; drought monitoring; drought analysis; agricultural drought; wet-environment evapotranspiration; WEAP; Lempa River basin; mutual information; ONI

Abstract

Drought is a major threat to global agriculture and can trigger or intensify food price increase and migration. Assessment and monitoring are essential for proper drought management. Drought indices play a fundamental task in this respect. This research introduces the Wet-environment Evapotranspiration and Precipitation Standardized Index (WEPSI) for drought assessment and monitoring. WEPSI is inspired by the Standardized Precipitation Evapotranspiration Index (SPEI), in which water supply and demand are incorporated into the drought index calculation. WEPSI considers precipitation (P) for water supply and wet-environment evapotranspiration (ET_w) for water demand. We use an asymmetric complementary relationship to calculate ET_w using actual (ET_a) and potential evapotranspiration (ET_p). WEPSI is tested in the transboundary Lempa River basin located in the Central American dry corridor. ET_w is estimated based on evapotranspiration data calculated using the Water Evaluation And Planning (WEAP) system hydrological model. To investigate the performance of our introduced drought index, we compare it with two well-known meteorological indices (Standardized Precipitation Index and SPEI), together with a hydrological index (Standardized Runoff Index), in terms of correlation and mutual information (MI). We also compare drought calculated with WEPSI and historical information, including crop cereal production and Oceanic Niño Index (ONI) data. The results show that WEPSI has the highest correlation and MI compared with the three other indices used. It is also consistent with the records of crop cereal production and ONI. These findings show that WEPSI can be applied for agricultural drought assessments.

1 Introduction

Drought affects around 40% of the global land area and is a major threat to global agriculture (Wang et al., 2011; Wen et al., 2021). It can trigger or intensify wildfire, water scarcity, crop damage, food price increase, migration, and adverse health impacts (Mukherjee et al., 2018). Drought monitoring is crucial to pre-prepare for drought and mitigate its negative effects. In this regard, drought indices are useful measures for scientists and decision makers to monitor, assess, and manage drought.

Although there exists no unique standard definition for drought, it is described as the deficit in precipitation (P) compared with an average within a period (Wang et al., 2020; Yihdego et al., 2019). The combination of anomalies in P and temperature, known as meteorological drought, leads to soil moisture deficit, referred to as agricultural drought, and a lack of water in lakes and streams, defined as hydrological drought (Mukherjee et al., 2018; Wilhite and Glantz, 1985). Agricultural and hydrological droughts are usually the subsequent phases of meteorological drought (Peters et al., 2003).

A drought index aims to quantify drought severity and help in the identification and characterization of drought development by assimilating a hydrometeorological dataset into numerical values that indicate the magnitude of water anomalies. Selecting a proper drought index for drought assessment and monitoring is not always trivial and involves different challenges. The following considerations should be made when selecting the drought index. (1) The drought index must follow the standardization of the hydrometeorological variable used. Otherwise, in contiguous regions, the same drought index can show different drought conditions, making it difficult to calculate drought onset and spatial extent. (2) It is preferable that the methodology for the calculation is clear and that the fewest possible inputs are used. Some drought indices are not usable every-where. Some others require many inputs or have complex structures that make their

implementation difficult. (3) It is desirable if the drought index can identify different types of droughts. Some drought indices can detect various types of droughts, making them have a broader range of applications (Yihdego et al., 2019).

Much academic effort has been devoted to introducing appropriate drought indices. As an early attempt, Palmer (1965) proposed a regional index to determine meteorological and agricultural droughts, known as the Palmer Drought Severity Index (PDSI). The PDSI uses temperature, soil moisture, and P. The structure of the PDSI does not allow for comparison across different regions. Time scale limitation and data complexity are also high-lighted deficiencies of the PDSI. Based on these drawbacks, three years later, Palmer introduced his Crop Moisture Index (CMI) for agricultural drought (Palmer, 1968). The self-calibrated Palmer Drought Severity Index (scPDSI), proposed by Wells et al. (2004), is another index based on the PDSI but allows comparison of different regions.

One of the most outstanding advances in developing drought indices was made by McKee et al. (1993). They proposed one of the most well-known drought indices, the Standardized Precipitation Index (SPI). The SPI is popular because of its simple structure. It can be calculated with the presence of missing data. The SPI has the flexibility of calculation in short or long time steps (aggregation periods), which is especially advantageous in monitoring different types of droughts (Vicente-Serrano et al., 2010; Yihdego et al., 2019). Nevertheless, the SPI overlooks the role of other important variables, such as evapotranspiration (ET) (Mukherjee et al., 2018; Vicente-Serrano et al., 2010), and it cannot reflect the in-crease in water demand because of temperature. In response to this limitation, Vicente-Serrano et al. (2010) introduced another widely used drought index, the Standardized Precipitation Evapotranspiration Index (SPEI). The SPEI uses the SPI's structure but applies temperature and P. This drought index can capture agricultural drought more efficiently than SPI can, as it uses potential evapotranspiration (ET_p) (Yihdego et al., 2019). However, the SPEI may face limitations when comparing drought across different climate regions (Mukherjee et al., 2018).

P is the basis for the calculation of many drought indices. At different time aggregations, P can help indicate all types of droughts. It is relatively the most direct variable of water supply (Yihdego et al., 2019). However, using only P leads to a failure to incorporate the changes in available energy, air humidity, and wind speed; consequently, it can provide values that do not capture reality (Mukherjee et al., 2018). Drought relies not only on water supply but also on water demand, for which ET can be the proxy (Speich, 2019). ET forces around 60% of the land P to return to the atmosphere (Zhang et al., 2020) and creates two-thirds of the planet's annual P. It also consumes more than half of the solar energy absorbed by the land surface as latent heat. Accordingly, ET, which contributes to mass and energy exchange between land and atmosphere (Zhang et al., 2020), is crucial in improving our vision of land-atmosphere interactions and the terrestrial water cycle (Xiao et al., 2020; Zheng et al., 2019). These explain ET's important role in releasing droughts (Mukherjee et al., 2018) and drought severity at both the local and global scales (Dhungel and Barber, 2018; Zhang et al., 2020). Therefore, using ET together with P in the structure of drought indices allows a more comprehensive drought assessment (Lu et al., 2019; Zargar et al., 2011).

ET has several types, and selecting its type is highly critical in defining the drought index. For instance, the so-called Standardized Precipitation Actual Evapotranspiration Index uses actual evapotranspiration (ET_a) in its structure (Homdee et al., 2016). However, the difference between P and ET_a could not capture the real water shortage (WS). This is because ET_a is not the ultimate

possible amount of ET but the real ET occurring on the surface (Kim and Rhee, 2016; Vicente-Serrano et al., 2018). As one of the other types of ET, ET_p , which has already been used in the structure of some drought indices in the literature, is a measure of atmospheric evaporative demand (Dash et al., 2021; Kim and Rhee, 2016; Vicente-Serrano et al., 2018; Yihdego et al., 2019). Wet-environment evapotranspiration (ET_w) is ET from an extensive, well-watered surface into the atmosphere (Aminzadeh et al., 2016; Kahler and Brutsaert, 2006).

To specify the appropriate water demand term for drought assessment, it is essential to be aware of both water balance and energy balance (Koppa et al., 2021). The literature in this area is rich, and among existing studies is the rigorous work conducted by Fisher et al. (2011), which has taken a proper look into the concept.

Based on water balance in a closed system (e.g., a watershed), where P is the only water supply, the supplied water takes one of the following forms (human systems, extraction by insects or animals, and leaking into the earth's deep crust are not part of this scope):

1) Going into the soil and Ground-Water flow or recharge (GW); 2) surface Runoff (R); 3) being Stored in lakes, ponds, and plants (S); and 4) going back to the atmosphere (ET_a). The water balance equation is expressed as follows:

$$P = GW + R + S + ET_a \quad (1)$$

The upper limit of ET_a in water balance is ET_w and will occur only if enough water is supplied (Fisher et al., 2011). ET_w changes by energy variation. Then, we can define water loss via ET as follows:

$$P - ET_a = GW + R + S \quad (2)$$

Apparently, we always have $P - ET_a \geq P - ET_w$.

Then, one can claim that ET_w illustrates the real ET demand.

Despite its important role as an indicator of water demand, the use of ET_w in the structure of P-based drought indices has been almost overlooked in the literature. Incorporating ET_w in drought index calculations, especially for agricultural purposes, is advantageous. It captures a more realistic condition in which the important role of ET as water demand is neither underestimated nor overestimated by using a pessimistic indicator.

As a robust and generalized drought index running through a simple structure is essential for improving water resource management and planning (Yihdego et al., 2019), this research introduces the Wet-environment Evapotranspiration and Precipitation Standardized Index (WEPSI). WEPSI is inspired by the SPEI, in which water supply and demand are incorporated into the drought index calculation. WEPSI follows the SPI methodology for its calculation, while P is considered for water supply and ET_w for water demand. Priestley and Taylor's model (P-T model) (Priestley and Taylor, 1972) is widely used as a proxy of ET_w (Kahler and Brutsaert, 2006). This model has a coefficient that was proposed to account for the drying power of the air, with an estimated mean value of 1.26 (or $\alpha = 1.26$) over saturated surfaces, such as oceans. Recent research has shown that this coefficient is impacted by the radiation regime, relative humidity, air temperature, wind speed, and geographical site. This raises doubts about the use of P-T model outputs without calibration of its coefficient (Aminzadeh and Or, 2014). Accordingly, we used an asymmetric Complementary Relationship (CR) to obtain ET_w using ET_a and ET_p , based on our reliable data (Khoshnazar et al., 2021a). To evaluate the performance of WEPSI, we first compared

its results with both well-known drought indices (SPI, SPEI), as well as with the Standardized Runoff Index (SRI). The coefficient of determination and mutual information (MI) were used for this comparison. Additionally, the fluctuation in cereal and crop production in El Salvador, as well as El Niño Southern Oscillation (ENSO) events, was compared to drought calculated using WEPSI, illustrating its performance, especially for agricultural purposes. We assessed WEPSI at the catchment scale using ET data calculated from the Water Evaluation And Planning (WEAP) system hydrological model.

The remainder of the paper is organized as follows. In Section 2, Materials and Methods, we start with our case study area. Then, the WEAP model and benchmark drought indices are provided. As the core of this section, WEPSI is introduced, and the experimental setup is presented. The results and discussion are given in Section 3. Finally, Section 4 concludes the paper and suggests directions for future research.

2 Materials and Methods

2.1 Case study

The transboundary Lempa River basin located in the Central American dry corridor is used as our case study area in investigating WEPSI. With a length of 422 km, the Lempa River is the longest stream in Central America. It originates from volcanic mountains in Guatemala, with 1,500 masl elevation, and flows to the Pacific Ocean in El Salvador. Around 360.2 km (85%) of the river's length flows into El Salvador's territory (Hernández, 2005). This river flows through Guatemala, Honduras, and El Salvador (Figure 1). The area of the tri-national basin is 17,790 km², of which 10,082 km² belongs to El Salvador (49% of El Salvadorian land). The basin has a daily average temperature of 23.5°C, a total annual rainfall average of 1,698 mm, and a yearly R of 19.21 dm³ s⁻¹ km².

The Lempa River streamflow has dropped by 70% (Helman and Tomlinson, 2018; Jennewein and Jones, 2016) during the dry years. This is while based on El Salvador's Ministry of Environment and Natural Resources (MARN) (2019b) data, El Salvador gains 68% of its surface water from this river basin. The basin environs 13 of 14 departments of El Salvador, including 3,967,159 inhabitants (77.5% of the country's population). Alterations in the hydrological regime, such as extreme events (e.g., drought and tropical cyclone), worsen water quality and quantity in the region (Global Environment Facility, 2019). The current condition of the basin highlights the need for water resource management and drought assessment.

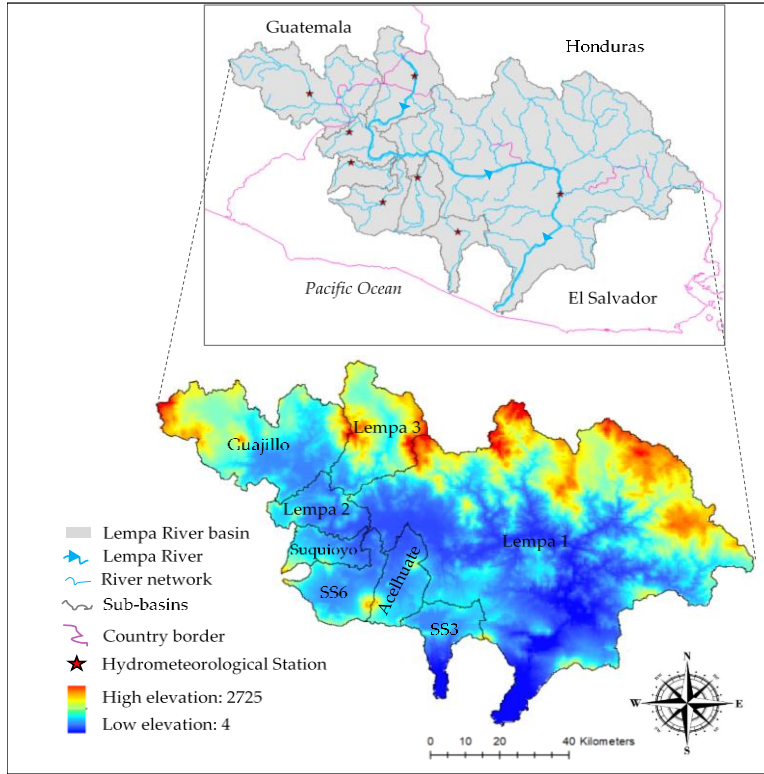


Figure 1. Lempa River basin location (Khoshnazar et al., 2021a).

2.2 WEAP model

The WEAP system is a well-known model for water resource planning developed by the Stockholm Environment Institute (Seiber and Purkey, 2015). WEAP allows the calculation of terrestrial hydrological cycle variables, such as R, infiltration, and ET. We used WEAP-derived ET to calculate WEPSI. The required input data on hydrometeorological and soil characteristics of the model were obtained from MARN (2019a), and the updated version of Sheffield et al. (2006) for the period 1980–2010. Based on basin management by local authorities and physiographic characteristics, the Lempa River basin was divided into the following eight sub-basins: Lempa 1, Lempa 2, Lempa 3, Guajillo, Suquioyo, Acelhuate, SS6, and SS3 (Figure 1). Khoshnazar et al. (2021a) showed that the WEAP-derived variables are reliable for drought assessment in the Lempa River basin. For the description of the validation and calibration procedure of the model, interested readers are referred to our previous publication (Khoshnazar et al., 2021a).

Five methods to simulate basin processes, such as ET, R, and irrigation demands, are available in WEAP. In our research, we use the soil moisture method, which considers that the basin has two soil layers (buckets or tanks). The top soil layer is considered shallow-water capacity, and the bottom soil layer is considered deep-water capacity. Figure 2 depicts a conceptual diagram of the soil moisture method (Seiber and Purkey, 2015). The water balance is calculated for each fraction area j for the first layer, assuming that the climate is steady in each sub-basin. The water balance is calculated using Eq. (3) as follows (Oti et al., 2020):

$$Rd_j \frac{dZ_{1,j}}{dt} = P_e(t) - ET_p(t)k_{c,j}(t) \left(\frac{5Z_{1,j} - 2Z_{1,j}^2}{3} \right) - P_e(t)Z_{1,j}^{RRF_j} - f_j k_{s,j} Z_{1,j}^2 - (1 - f_j) k_{s,j} Z_{1,j}^2 \quad (3)$$

where $Z_{1,j}$ is the relative storage based on the total effective storage of the root zone. Rd_j is the soil holding capacity of the land cover fraction j (mm). ET_p is calculated using the modified Penman–Monteith reference crop ET_p with the crop/plant coefficient ($k_{c,j}$). P_e is the effective precipitation (P), and RRF_j is the R resistance factor of the land cover. $P_e(t)Z_{1,j}^{RRF_j}$ is indicated as the surface R. $f_j k_{s,j} Z_{1,j}^2$ shows the interflow from the first layer, for which the term $k_{s,j}$ denotes the root zone saturated conductivity (mm/time), and f_j is the partitioning coefficient that considers water horizontally and vertically based on the soil, land cover, and topography. Finally, the term $(1 - f_j)k_{s,j} Z_{1,j}^2$ is percolation. WEAP uses Eq. (4) to calculate ET_a (Kumar et al., 2018):

$$ET_a = ET_p \frac{(5z_1 - 2z_2^2)}{3} \quad (4)$$

where z_1 and z_2 are the water depth of the top and bottom soil layers (bucket), respectively (Figure 2).

We calculated the monthly ET_w with the WEAP-derived ET_p and ET_a following the procedure presented in Section 2.4.2 for each sub-basin.

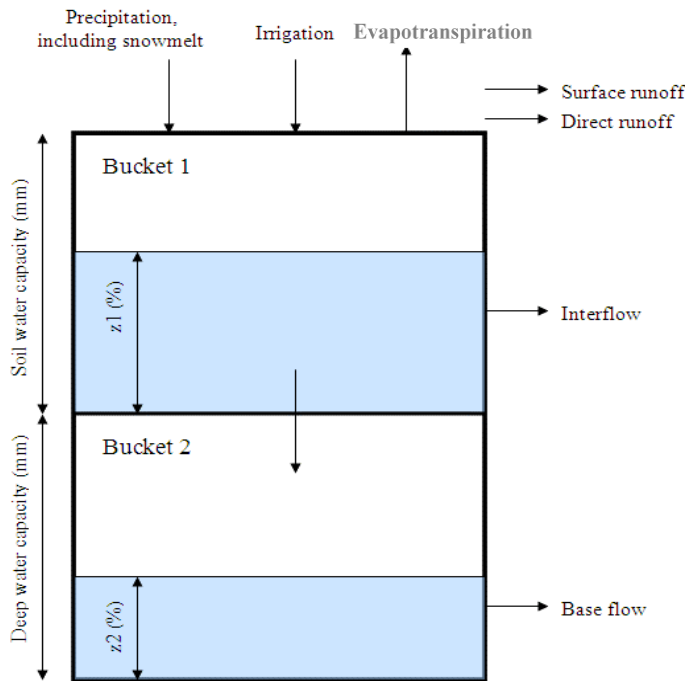


Figure 2. Conceptual diagram of the water balance calculation in WEAP (Seiber and Purkey, 2015).

2.3 Drought indices for comparison

We compare SPI and SPEI meteorological drought indices with WEPSI. As discussed, SPI is based on the total amount of water (i.e., P), whereas SPEI incorporates the reduction of water based on ET_p . Then we compare these three indices (SPI, SPEI, and WEPSI) with SRI, which is a hydrological drought index and reflects the real water availability on land. The application of a hydrological drought index can provide us with further insights into the situation of the studied area compared with using only meteorological drought indices (Shukla and Wood, 2008). On the

other hand, based on the water balance equation, SRI implicitly reflects ET_a (Vicente-Serrano et al., 2010). Accordingly, when a meteorological drought index reflects a high similarity with SRI, it provides more insights into the hydrological situation of the land and is closer to the real evapotranspiration condition. Such an index has a higher potential to be used solely without requiring a complementary hydrological index and, consequently, eliminates the difficulty of gathering and modeling hydrological data.

The methodology for calculating these drought indices is as follows.

2.3.1 The Standardized Precipitation Index (SPI)

The methodology for calculating the SPI is presented as follows (McKee et al., 1993). Based on long-term P data (30 years or more), a time scale (also known as aggregation period) is specified. This time scale can be 3, 6, 9, 12, 24, or 48 months. Then, the aggregated P is fitted to a distribution function. Afterward, the cumulative probability function is equal to that of the normal distribution, for which the standardized variable with zero mean and unity standard deviation is obtained. The literature suggests the Gamma distribution as one of the best choices for SPI calculation (Kim et al., 2019; McKee et al., 1993). Therefore, we have used Gamma distribution for SPI calculation, as well.

2.3.2 The Standardized Precipitation Evapotranspiration Index (SPEI)

The SPEI follows the SPI methodology but uses the difference between P and ET_p as its input (Vicente-Serrano et al., 2010). Several studies have shown that the log-logistic distribution is appropriate for SPEI calculation (Vicente-Serrano et al., 2010). Accordingly, we have used the three-parameter log-logistic (LL3) distribution for obtaining the SPEI.

2.3.3 The Standardized Runoff Index (SRI)

The SRI uses R as input and follows a similar procedure as SPI (Shukla and Wood, 2008). McKee et al. (1993) proposed a gamma distribution for the SPI and suggested that this distribution is operational for other variables related to drought (Sorí et al., 2020). Accordingly, we have used the Gamma distribution to calculate SRI, utilizing R data obtained from the WEAP model.

2.4 The Wet-environment Evapotranspiration and Precipitation Standardized Index (WEPSI)

2.4.1 WEPSI calculation

WEPSI is calculated following the SPI methodology to standardize the input, except that WEPSI uses WS instead of P alone.

WS is calculated as the difference between P (water supply) and ET_w (water demand) (Eq. (5)).

$$WS = P - ET_w \quad (5)$$

WEPSI is inspired by the structure of the SPEI that uses ET_p to incorporate water demand into the drought index calculation. Based on our discussions in the previous section, ET_w can be an appropriate representative of water demand. Accordingly, we incorporate ET_w into WEPSI as the water demand indicator and P to account for the water supply. Since WEPSI incorporates $P - ET_w$ as its input and concerning the water balance equation (Eq. (1)), we anticipate that our

proposed drought index should have a higher correlation with SRI and, therefore, can provide useful information about the hydrological situation of the area. We will later investigate this in the numerical results.

As LL3 distribution has shown good performance in SPEI calculation and similar drought indices, we consider LL3 distribution to fit WS in WEPSI calculation (Kim and Rhee, 2016; Vicente-Serrano et al., 2010). Similar to SPI, WEPSI can be obtained based on different time steps, such as 3, 6, 9, 12, 24, and 48 months.

Since WEPSI follows the structure of the SPI, we consider the same drought categorical classification (Table 1).

Table 1. Drought categorical classification using WEPSI

WEPSI value	Drought/Wet category
≥ 2	Extreme wet
1.5 to 2	Severe wet
1 to 1.5	Moderate wet
0 to 1	Low wet
-1 to 0	Low drought
-1.5 to -1	Moderate drought
-2 to -1.5	Severe drought
≤ -2	Extreme drought

ET_w used in Eq. (5) is calculated based on the methodology introduced in the following subsection.

2.4.2 ET_w calculation

As previously mentioned, we have used CR to obtain ET_w data. Based on the Bouchet hypothesis (Bouchet, 1963), equilibrium evapotranspiration or ET_w is equal to ET_a and ET_p under saturated conditions. A saturated condition refers to an extensive, well-watered surface where input energy is the limiting factor (Xiao et al., 2020). We always have $ET_a \leq ET_w$ and $ET_p \geq ET_w$. ET_w , ET_p , and ET_a have been related to one another by what is known as CR. A general form for CR is suggested by Kahler and Brutsaert (2006) (Eq. (6)).

$$(1 + b)ET_w = bET_a + ET_p \quad (6)$$

where b is an empirical constant, and ET_a , ET_p , and ET_w are the actual, potential, and wet-environment evapotranspiration, respectively.

The symmetric CR considered by Bouchet is obtained by taking $b = 1$ in Eq. (6). However, the literature indicates that b generally exceeds and is rarely equal to 1 (i.e., CR is asymmetric) (Aminzadeh et al., 2016). Consequently, for the ET_w calculation, in addition to ET_p and ET_a , it is necessary to estimate the value of b .

Eq. (6) can be rewritten in terms of b (Aminzadeh et al., 2016).

$$b = \frac{ET_p - ET_w}{ET_w - ET_a} \quad (7)$$

Eq. (7) shows that the increase in ET_p above ET_w is proportional to the energy flux provided by surface drying and the decrease in evaporation rate.

Normalizing Eq. (7) results in Eq. (8) and Eq. (9) (Aminzadeh et al., 2016),

$$ET_{a+} = \frac{(1+b)ET_{MI}}{1+bET_{MI}} \quad (8)$$

$$ET_{p+} = \frac{1+b}{1+bET_{MI}} \quad (9)$$

where $ET_{a+} = \frac{ET_a}{ET_w}$, $ET_{p+} = \frac{ET_p}{ET_w}$, $ET_{MI} = \frac{ET_a}{ET_p}$, and ET_{MI} is the surface moisture index (with a maximum of 1). ET_{a+} and ET_{p+} are the scaled actual and potential evapotranspiration with respect to different values of the surface moisture index.

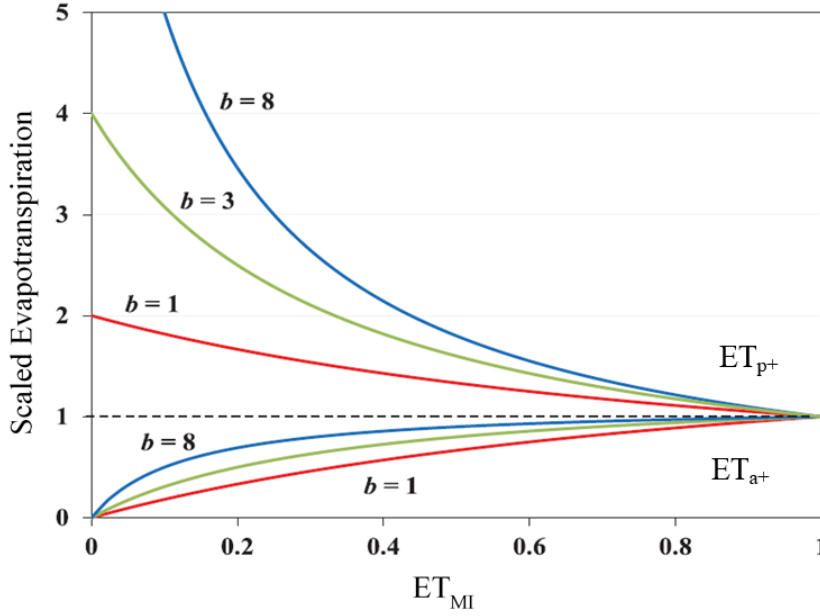


Figure 3. Scaled actual (ET_{a+}) and potential evapotranspiration (ET_{p+}) with respect to the surface moisture index (ET_{MI}) variations for different values of b (Aminzadeh et al., 2016; Kahler and Brutsaert, 2006).

The b parameter in Eq. (8) and (9) can be obtained from Eq. (10) (Aminzadeh et al., 2016; Granger, 1989; Xiao et al., 2020),

$$b = \frac{1}{\gamma} \frac{e_s^* - e_w^*}{T_s - T_w} \quad (10)$$

where e_s^* is the saturated vapor pressure at surface temperature T_s , and e_w^* is the saturated vapor pressure at a hypothetical wet surface temperature T_w . The psychrometric constant γ (in $\text{kPa } ^\circ\text{C}^{-1}$) is calculated with the atmospheric pressure (P_e) as $\gamma = 0.665 \times 10^{-3} P_e$, with P_e in kPa .

Alternatively, to facilitate the calculation of CR, Aminzadeh et al. (2016) suggested an atmospheric input-based equation for b (Eq. (11)), which is more straightforward than Eq. (10) (Han and Tian, 2020); this is why we have used this equation in our paper.

$$b = A R_{S,net} + B \quad (11)$$

where $R_{S,net}$ is the net shortwave radiation flux in W m^{-2} . $R_{S,net}$ is calculated with the incoming shortwave radiation flux RS and the surface albedo α as $R_{S,net} = (1 - \alpha)R_S$.

A is a function of wind speed u_a (in m.S^{-1}) (Eq. (12)).

$$A = (3u_a + 2) \times 10^{-3} \quad (12)$$

Finally, the B parameter is calculated as a function of wind speed (u_a) and vapor concentration (c_a (kg m^{-3})) (Eq. (13)).

$$B = (24.3 u_a - 1.44)(c_a + 22 \times 10^{-3}) + 0.3 \quad (13)$$

To calculate b using Eq. (11), $R_{S,\text{net}}$, u_a , and c_a are required, which can be obtained from meteorological measurements, the literature, or empirical equations.

2.5 Experimental setup

2.5.1 WEPSI calculation at the catchment scale

WEPSI is applied in the Lempa River basin; we have calculated it for each sub-basin (Section 2.1). Eq. (6) is used to obtain ET_w .

To derive ET_w from Eq. (6), we first applied Eq. (11) to calculate parameter b for 12 months of the year in each sub-basin. In this order, the daily datasets of wind speed (u_a), net shortwave radiation ($R_{S,\text{net}}$), and vapor concentration (c_a) for 31 years (1980–2010) and for each sub-basin are used to calculate the monthly average of these three inputs. The meteorological data u_a , $R_{S,\text{net}}$, and c_a were retrieved from MARN (2019a) and Khoshnazar et al. (2021a). The ranges of the obtained b values are validated by comparing them with the values available in the literature (Aminzadeh et al., 2016).

After obtaining b , we used the time series of WEAP-derived ET_p and ET_a (Section 2.2) as the inputs of Eq. (6) to calculate ET_w in each sub-basin.

Finally, with the catchment-wide P and ET_w , we computed WEPSI for the time steps 3, 6, 9, and 12 months, which are indicated as WEPSI03, WEPSI06, WEPSI09, and WEPSI12, respectively.

2.5.2 WEPSI performance evaluation

To compare WEPSI in calculating drought, we have used SPI and SPEI, two vastly applied meteorological drought indices. In drought studies, the SPEI has also been applied to agricultural drought assessments. We further utilized the SRI as a hydrological drought index to investigate whether WEPSI could provide insights into the hydrological situation. For the calculation of the SPI, SPEI, and SRI, we followed the methodology presented in Section 2.3. The catchment-wide P , ET_p , and R derived from the WEAP model were the inputs used to compute the drought indices for each sub-basin. These three drought indices were similarly calculated for the time steps 3, 6, 9, and 12 months. The same notation used in WEPSI is utilized in this case. Therefore, for instance, the 6-month time step for the SPI, SPEI, and SRI is indicated as SPI06, SPEI06, and SRI06, respectively.

The comparison is carried out in the following steps. First, a metric commonly used in the performance evaluation of drought indices is applied to compare WEPSI, SPI, SPEI, and SRI, which is the coefficient of determination (r^2) calculated using Eq. (14) as follows:

$$r^2 = \left(\frac{\sum_{i=1}^n (x_i - \bar{x})(y_i - \bar{y})}{\sqrt{\sum_{i=1}^n (x_i - \bar{x})^2 \sum_{i=1}^n (y_i - \bar{y})^2}} \right)^2 \quad (14)$$

where x_i and y_i indicate the reference variable and the variable to compare, respectively, and \bar{x} and \bar{y} indicate the mean of such values.

Second, we use the concept of MI to complement our evaluation, where MI is calculated between WEPSI, SPI, SPEI, and SRI. MI is calculated between two variables to determine the amount of information one variable has about the other (Vergara and Estévez, 2014). This concept is valuable in our comparison procedure, as we seek to know how much information is available about the others in each drought index. MI is calculated using Eq. (15) (Interested readers are referred to (Vergara and Estévez, 2014) and (Al Balasmeh et al., 2020) for the theoretical background underlying the calculation of MI).

$$MI(x; y) = H(x) - H(x|y) = \sum_{i=1}^n \sum_{j=1}^n p(x(i), y(j)) \cdot \log \left(\frac{p(x(i), y(j))}{p(x(i)) \cdot p(y(j))} \right) \quad (15)$$

where $MI(x; y)$ is the MI between variable x and y , $H(x)$ is the entropy of a discrete random variable x , $H(x|y)$ is the conditional entropy of two discrete random variables of x and y , $p(x)$ denotes the probability of the random variable x , and $p(x, y)$ is the joint probability of the random variables of x and y . MI is zero if x and y are statistically independent, and $MI(x; y) = MI(y; x)$.

The unit of information or entropy is nat (natural unit of information), which is based on natural logarithms and powers of e instead of the base two logarithms and powers of two used in the bit unit.

Figure 4 shows the Venn diagram based on Eq. (15), which schematizes the relationship between MI and entropies (H) between the random variables x and y .

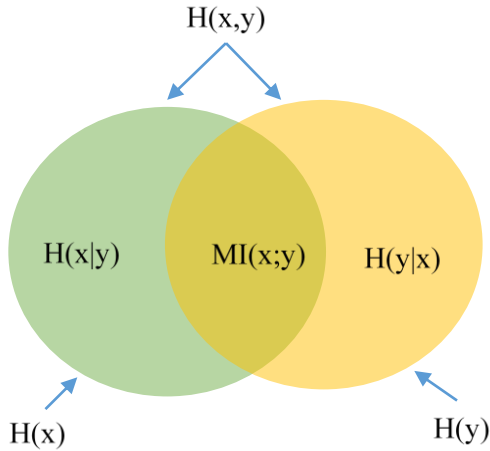


Figure 4. Venn diagram of the relationship between mutual information (MI) and entropy (H).

As drought is an important environmental driver that leads to cereal loss in both yield and quality worldwide (Karim and Rahman, 2015), we also compare the cereal production data of El Salvador with the results of the drought indices in this research.

With the time series of WEAP-based WEPSI calculated in each sub-basin, we compute the time series of the percentage of drought area (PDA) for the entire basin. PDAs were calculated monthly as the ratio between the area of sub-basins in drought and the total area of the basin. A drought event starts once the drought index value goes below a threshold and ends as the value rises above the threshold again (Brito et al., 2018; Corzo et al., 2018; Corzo Perez et al., 2011; Diaz et al., 2020). The threshold used in this application was drought index = -1 , which is a threshold commonly used in drought assessments (Diaz et al., 2020; Khoshnazar et al., 2021a).

Finally, we compared PDA fluctuations with El Niño–La Niña years and with El Salvadorian cereal production. Cereal production is used because a lack of soil moisture can lead to a severe reduction in cereal production. On the other hand, drought causes yield and quality loss of cereal globally. Then, if WS, and thereby WEPSI, can capture the status of soil moisture and drought, there should exist a relationship between WEPSI and cereal production (Khoshnazar et al., 2021a; Lewis et al., 1998).

3 Results and discussion

3.1. WEPSI calculation and performance evaluation

CR was used to calculate the ET_w dataset as follows. The b parameter was calculated following the methodology presented in Section 2.4.2 for 12 months in eight sub-basins. Figure 5 depicts the asymmetric CR between ET_{a+} and ET_{p+} as functions of ET_{MI} for 12 months of the year in the Guajillo sub-basin. This figure also shows the symmetric CR that would occur if b was equal to 1. As Figure 5 illustrates, compared with the symmetric CR, the calculated b leads to a considerable difference between the scaled evapotranspiration (ET_{a+} and ET_{p+}) as the surface dries and ET_a decreases (Aminzadeh et al., 2016). Figure 5 also highlights the importance of using local and temporal meteorological data (net shortwave radiation, wind speed, and vapor concentration), which can lead to a more accurate approximation of CR and, consequently, of ET_w .

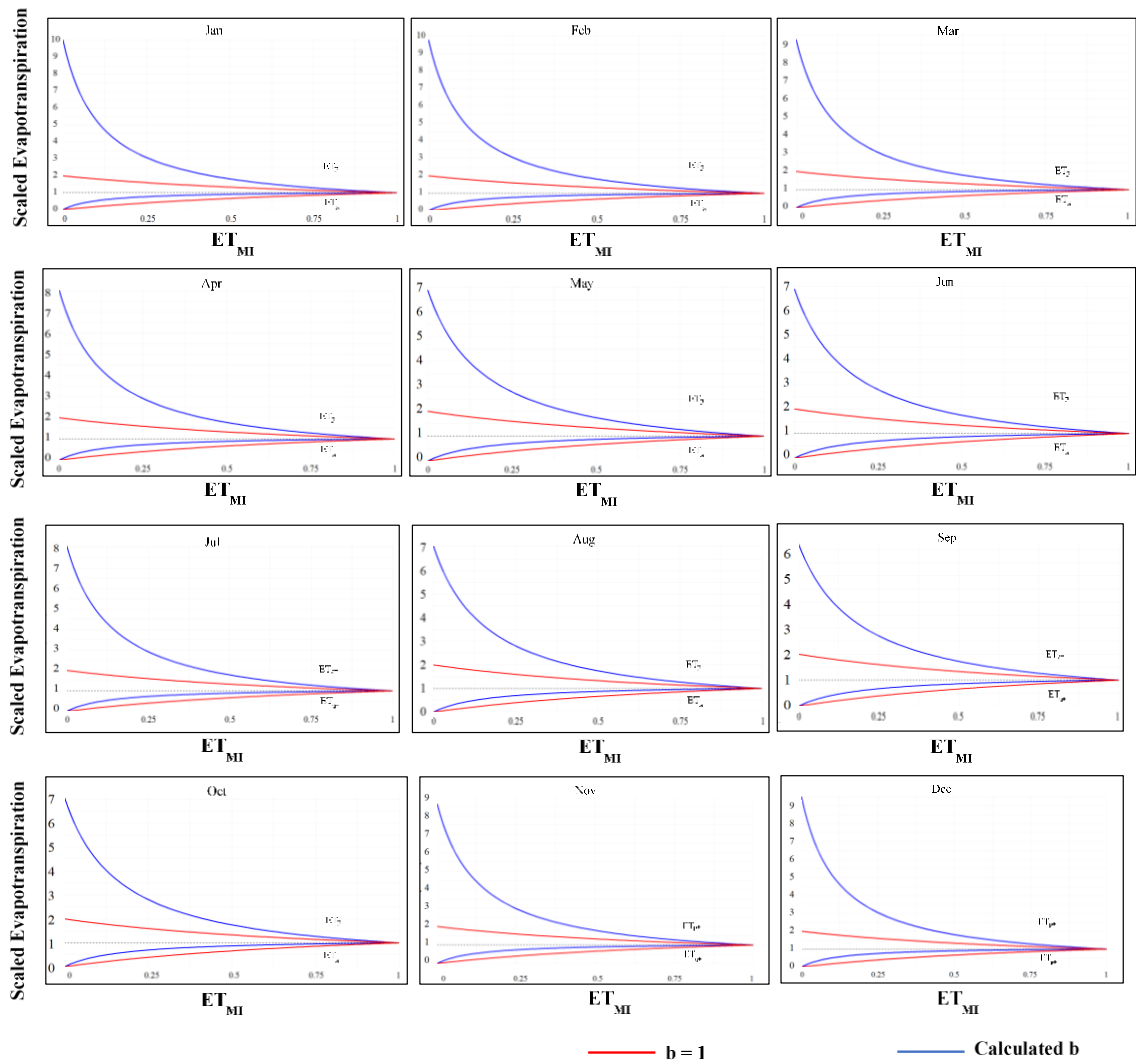


Figure 5. Scaled actual (ET_{a+}) and potential evapotranspiration (ET_{p+}) with respect to the surface moisture index (ET_{MI}) in the Guajillo sub-basin for 12 months of the year.

Figure 6 shows the time series of SPI06, SPEI06, SRI06, and WEPSI06 in the Guajillo sub-basin as an example of the calculation of the drought indices.

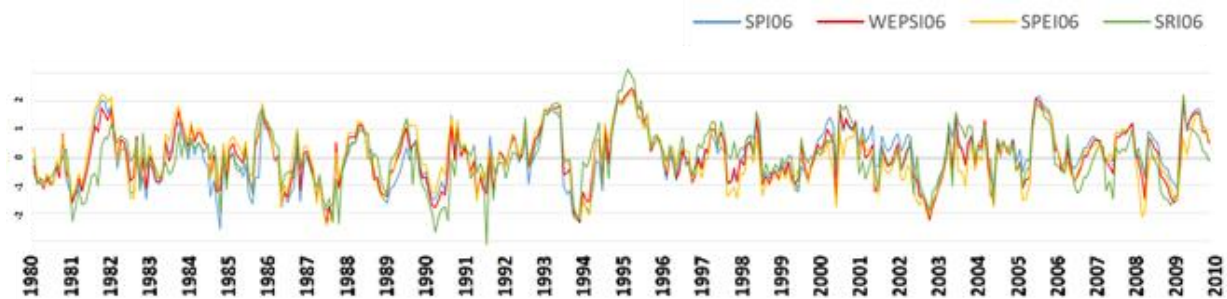


Figure 6. SPI06, SPEI06, SRI06, and WEPSI06 time series based on the WEAP-derived ET data for the Guajillo sub-basin (1980–2010).

Our results demonstrate that in 61% of the cases, the value of WEPSI06 is larger than that of SPEI06 (i.e., SPEI depicts a worse situation than WEPSI). The findings indicate that this behavior of WEPSI is observed among all other sub-basins, as well.

The literature states that an SPI with 3- or 6-month steps can be considered as an agricultural drought index (Khoshnazar et al., 2021a; McKee et al., 1993; Vicente-Serrano, 2006). It is also shown that SPI and SPEI, with 6-month time steps, have the highest correlation with each other (Diaz Mercado et al., 2018). Additionally, we compared the river streamflow with WEPSI and SRI for 3-, 6-, 9-, and 12-month time steps. We found that WEPSI06 and SRI06 were most related in terms of low flow in the basin. Accordingly, we consider WEPSI06 representative of the agricultural and hydrological drought conditions in the basin—WEPSI06 reflected a realistic vision of the basin that links meteorological, agricultural, and hydrological drought.

The correlation among the four drought indices is presented in Table 2. These correlations are the averages of the eight sub-basins. The correlations between WEPSI06 and SPI06 (0.931), WEPSI06 and SPEI06 (0.904), and WEPSI06 and SRI06 (0.783) are the highest. In comparison with the other drought indices, WEPSI has the highest correlation with all drought indices, and the correlation between SPEI06 and SRI06 (0.501) is the lowest.

Table 2. Correlation analysis

Drought indices	SPI06	SPEI06	SRI06	WEPSI06
SPI06	1	0.741	0.634	0.931
SPEI06	0.741	1	0.501	0.904
SRI06	0.634	0.501	1	0.783
WEPSI06	0.931	0.904	0.783	1

In addition to correlation analysis, MI was calculated among the drought indices (Section 2.6.2). As mentioned, MI was calculated to identify which drought index contains more information about the others. MI is expressed in nat, the International System of Units unit for entropy (details in Section 2.6.2).

Figure 7 depicts Venn diagrams that provide MI between drought indices. The values presented in Figure 7 are the averages of the eight sub-basins. The highest MI is between WEPSI06 and SPI06, WEPSI06 and SPEI06, and WEPSI06 and SRI06, with 0.74, 0.69, and 0.54 nat, respectively. The lowest MI is observed between SPEI06 and SRI06 (0.18 nat). The MIs between SPI06 and SPEI06, and SPI06 and SRI06 are 0.31 and 0.24 nat, respectively. Accordingly, WEPSI06 not only contains the highest amount of information about the two other meteorological drought indices (SPI06 and SPEI06) but also covers the most information about the hydrological conditions of the region (SRI06). SPEI06 and SPI06 send the lowest number of hydrological signals in terms of drought. The results of the correlation analysis and MI suggest that WEPSI is a drought index that identifies hydrological drought in the absence of R data.

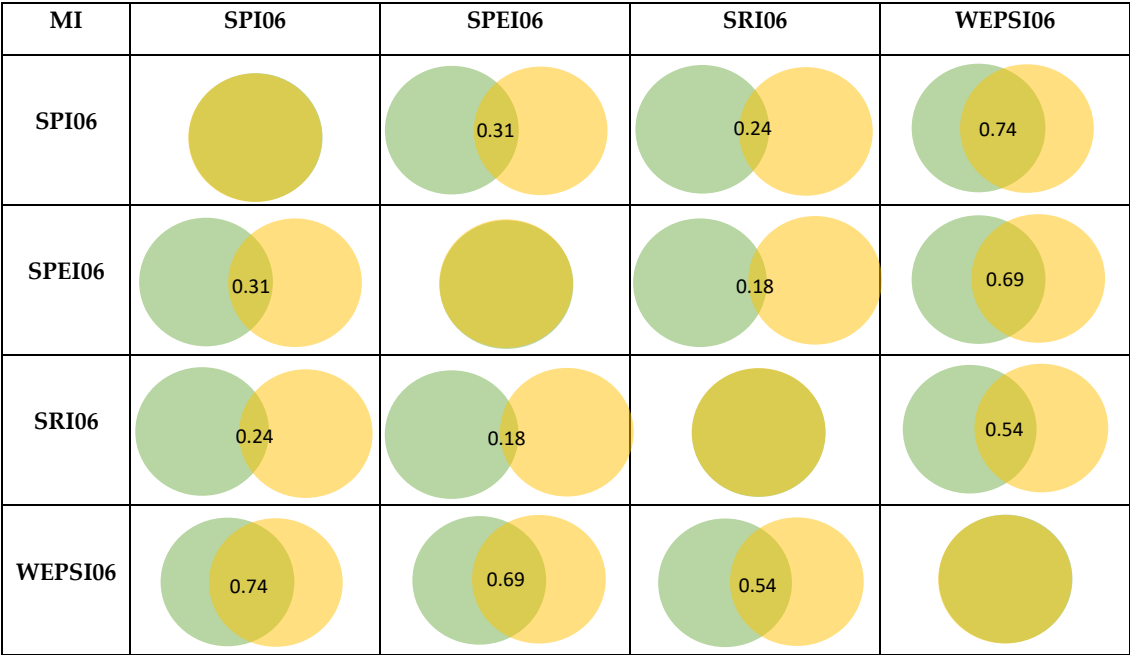


Figure 7. Mutual information (MI) Venn diagram between SPI06, SPEI06, SRI06, and WEPSI06. The intersection between two circles depicts the MI between two drought indices in nat, the SI unit for entropy.

Figure 8a–h compares the time series of the WEAP-based WEPSI06 in the eight sub-basins of the Lempa River basin for the period 1980–2010 (31 years). Based on Figure 8, the longest drought (i.e., number of months in which the value of WEPSI is below the threshold of -1) occurred in 2003, in general. The maximum drought frequency (3.54%) occurred in the Guajillo, SS6, and Suquioyo sub-basins, with a total of 13 droughts over 31 years. The most severe drought (i.e., aggregation of WEPSI values in sequent months at drought) occurred in Guajillo in December 1994.

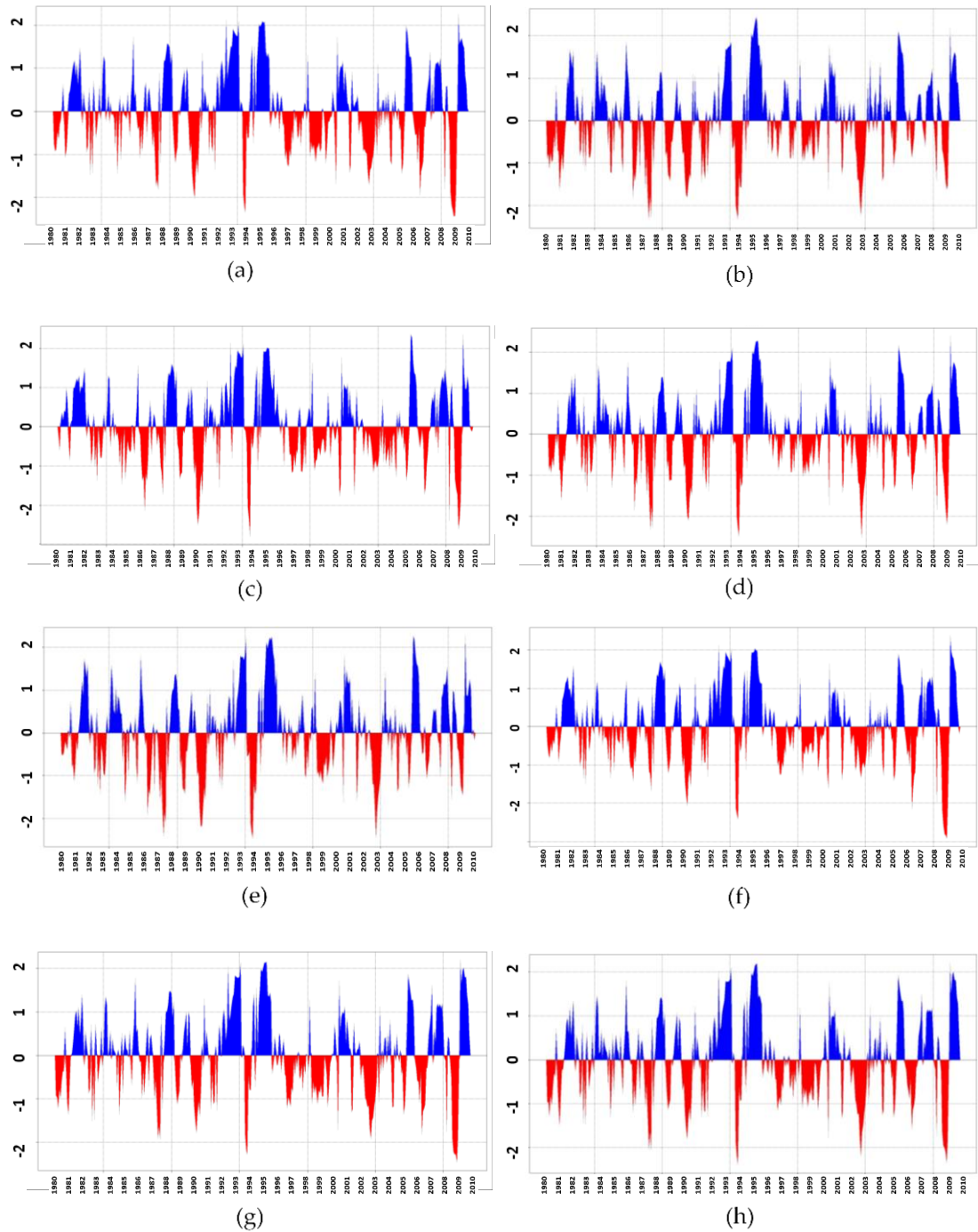


Figure 8. Time series of WEPSI06 in the sub-basins: (a) Acelhuate, (b) Guajillo, (c) Lempa 1, (d) Lempa 2, (e) Lempa 3, (f) SS3, (g) SS6, and (h) Suquioyo.

Figure 9 displays the variation of drought areas through the PDAs in the Lempa River basin for 31 years based on WEPSI06. The threshold of -1 was used to calculate drought in each WEPSI time series (i.e., a sub-basin is in drought if $\text{WEPSI06} \leq -1$; Table 1). Figure 9 shows some repetitive patterns in the behavior of droughts in the basin. Some years are in white cells, indicating the absence of PDA in those years, which are known as white years. By contrast, some other years show a tail (i.e., PDA occurs in some sequenced months, indicating long drought events).

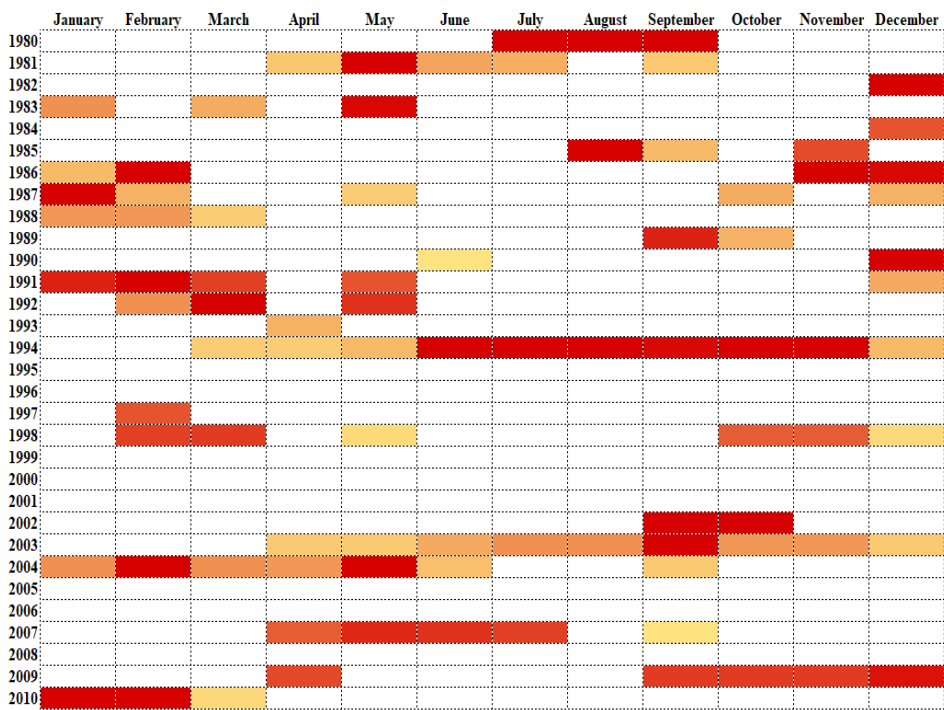


Figure 9. Percentage of drought area (PDA) using WEPSI06 based on WEAP data in the Lempa River basin for the period 1980–2010.

As ENSO events are usually linked to major flood and drought episodes (Mera et al., 2018), we have applied this information to assess the performance of WEPSI. Drought events indicated by the PDA results (Figure 9) are compared with the EL Niño and La Niña years based on the Oceanic Niño Index (ONI) (National Oceanic and Atmospheric Administration, 2015). ENSO events affect people and ecosystems across the globe via the production of secondary results that influence food supplies and prices, as well as forest fires, and create additional economic and political consequences (National Oceanic and Atmospheric Administration, 2015). Comparing the patterns of PDA based on WEPSI06 (Figure 9) and ONI shows that PDA shares similarities with La Niña in terms of white years, including weak La Niña in 1984, 2001, 2005, and 2006, moderate La Niña in 1995, 1996, 2000, and 2008, and strong La Niña in 1999. On the other hand, investigating the years with a drought tail reveals weak El Niño in 1980, 2004, 2007, 2009, and 2010, moderate El Niño in 1986, 1994, 2002, and 2003, strong El Niño in 1987, 1988, 1991, and 1992, and very strong El Niño in 1998. The consistency of the results provided by WEPSI06 with El Niño and La Niña years emphasize the good performance of WEPSI.

The fluctuation in cereal and crop production in El Salvador is shown in Figure 10 for the period 1980–2010 (31 years) (World Bank Group, 2021).

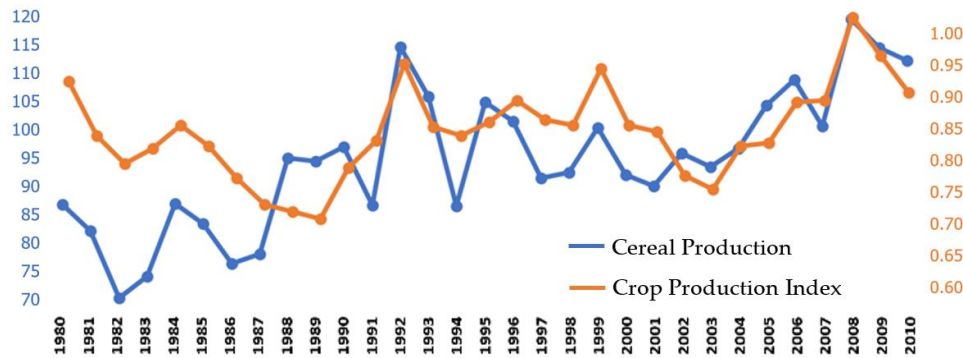


Figure 10. Cereal production (million metric tons) and crop production index in El Salvador for the period 1980–2010 (31 years) (Khoshnazar et al., 2021a).

As Figure 10 depicts, in 1984, 1988, 1990, 1992, 1995, 1999, 2002, 2006, and 2008, cereal production presented the local maximum amount compared with that in previous and subsequent years. On the other hand, the years 1982, 1986, 1989, 1991, 1994, 1997, 2001, 2003, and 2007 presented the local minimum. These years with the local minimum and maximum, aside from the years with descending and ascending cereal production amounts (compared with the previous year), were used for the comparison with drought indices' PDA. Our results endorse that the PDA of WEPSI06 based on WEAP model data detects six of the nine local maximums in El Salvador's cereal production evolution (when a year does not have at least two sequent months with a PDA value greater than 0% based on the drought index, and that year has a local maximum in the cereal production graph, the drought index is detecting the local maximum of cereal production), as well as six of the nine local minimums in cereal production fluctuation (when a year has some consecutive months with a PDA value greater than 0% based on the drought index, and that year has a local minimum in the cereal production graph, the drought index is detecting the local minimum of cereal production). This is while both SRI06 and SPEI06 detect four of the nine local maximums. SRI06 identifies five of the nine and SPEI06 reflects four of the nine local minimums of the graph. Finally, SPI06 does not detect a considerable number of critical points (i.e., the local maximum and minimum points) in El Salvador's cereal production graph. Besides, PDA based on WEPSI06 detects five years—1980, 1981, 1985, 2009, and 2010—when the tail of drought (at least two sequent months with a PDA greater than zero) is observed in them, and the amount of cereal production is lower than the previous year (i.e., the cereal production graph is descending); it also identifies that in 2005, which is a white year, the cereal production graph is ascending.

Generally, a growing pattern in cereal and crop production is observed during our study horizon. This is because cereal and crop productions do not depend on drought alone but are also influenced by other factors, such as agricultural land and technology. For example, El Salvador's agricultural land grew from 14,100 km² (or 68.05% of the land area) in 1980 to 15,350 km² (or 74.08% of the land area) in 2010 (Khoshnazar et al., 2021a). There are some other descriptions for the rise or drop in the cereal production graph. For example, 1992 has a tail of drought in Figure 9, while it has a local maximum in Figure 10. That is because 1992 was the end of the civil war in El Salvador, which affected the agricultural activity and production of the country. Moreover, in 1997, which is a white year with a local minimum in Figure 10, a surge in coffee prices led to the replacement of other products with coffee and a drop in cereal production. By contrast, the poor harvests and falling prices (around 50%) of coffee in that year altered farming decisions, giving

rise to a local maximum in 1998 (in Figure 9), while the tail of drought was also observed in that year in Figure 10 (Encyclopedia of the Nations, 2021).

As Figure 10 shows, the ascent and descent of the crop and cereal production graphs are the same except in 1987 and 1988, when the crop graph is descending but the cereal graph is ascending. There should be another probable occurrence or policy justifying this behavior of the cereal production graph, while these years have a tail of drought in Figure 9. Furthermore, the agricultural industry in El Salvador reported heavy losses because of rainfall and its consequences, such as flood and supersaturation within our study horizon (Freshplaza, 2021). This can justify the drop in cereal production in white years by PDA based on WEPSI06. For instance, in 1982, hurricane Paul killed 1,625 people and caused \$520 million in damage in Central America, including El Salvador. Similarly, hurricane Pauline in 1997 and tropical storm Arlene in 1993 impacted our studied basin (Carroll, 1998).

To sum up, PDA, based on WEPSI06, detects 85% of the cereal production drop and 70% of the cereal production increase. Taking the discussed abnormal conditions into account, the PDA based on WEPSI06 (Figure 9) is 81% consistent with the cereal production graph (Figure 10).

Regarding cereal production, the period between the first of April and the end of July is the lean period in the El Salvador cereal calendar based on Food and Agriculture Organization (FAO) of the United Nations (UN) (2021). Figure 9 demonstrates that tails of drought are observed in the lean period of cereal crops in El Salvador—during 1981, 1994, 2003, and 2007, when a reduction in cereal production also emerges. Additionally, the growing season, which starts from June and lasts until December (FAO, 2021), is also sensitive to WEPSI time-series droughts, as shown by the decrease in cereal production. This sensitivity to drought, similar to Daryanto et al.'s (2017) statement, is observed in 10 years in Figure 10. On the other hand, as the structure of WEPSI uses ET data, it implicitly determines soil moisture variability and, therefore, vegetation water content, directly affecting agricultural droughts (Vicente-Serrano et al., 2010). Indices that do not consider the role of temperature, and, consequently heat, could not depict the impact of this critical environmental component on crop survival, distribution, and productivity limits (Daryanto et al., 2017). This is while WEPSI implicitly takes the role of temperature into account and thus could be used for agricultural targets.

These observations indicate that the results of WEPSI06 could be used for the assessment of agricultural drought.

3.2 Significance of this study

Because of its inputs, WEPSI can indirectly take the climate change effect into account. WEPSI softens the performance of the SPEI because it uses ET_w instead of evaporative demand (i.e., ET_p). Accordingly, WEPSI can detect some events that are not captured by the SPI but can eliminate some others indicated by the SPEI that are derived by excessive values of ET_p .

Meteorological drought indices, such as the SPI and SPEI, describe climatic anomalies without considering their hydrologic context (Kim and Rhee, 2016). Hydrological drought indices, such as the SRI, represent the impact of climate anomalies on present hydrologic conditions, as they are controlled by physical processes on the surface (Shukla and Wood, 2008). Our results show a high correlation and MI between WEPSI06 and SRI06. These results indicate that WEPSI can depict a more accurate land surface status by linking meteorological and hydrological drought indices.

ET affects R (Vicente-Serrano et al., 2010), so the SRI can depict ET_a indirectly. Then, WEPSI, which, on the one hand, relatively reflects the SRI status and, on the other hand, uses ET, can indicate moisture conditions on the land surface. Additionally, our results showed a high similarity between the SRI with the 6-month time step (SRI06) and the Lempa River streamflow, suggesting that SRI06 reflects the basin's most accurate condition. The results again indicate that WEPSI can be used for agricultural drought assessments.

The proposed WEPSI drought index meets all requirements suggested by Nkemdirim and Weber for a drought index (Nkemdirim and Weber, 1999; Vicente-Serrano et al., 2010), including its use for different purposes. Drought characteristics, such as drought severity, intensity, and duration (the start and the end of the phenomenon), can also be calculated with WEPSI. Furthermore, WEPSI can be calculated worldwide and under various climates and can provide a spatial and temporal depiction of drought variation.

4 Conclusions

This research introduced WEPSI, which uses WS as its input. WS is calculated using P and ET_w . We embed ET_w into the structure of WEPSI to account for the water demand and P for the water supply. This paper also presents a procedure for ET_w calculation based on the asymmetric CR that links ET_p , ET_a , and ET_w .

We tested WEPSI in the Lempa River basin, which is the longest river in Central America. The basin is sub-divided into eight sub-basins for its modeling with the WEAP system. ET_w is calculated with ET_p and ET_a derived from WEAP.

We compared WEPSI with two meteorological drought indices (SPI and SPEI) and a hydrological drought index (SRI) via data derived from WEAP. The performance evaluation procedure includes a correlation coefficient (r) and an approach based on MI. The results show that WEPSI has the highest r and MI compared with the three other indices, indicating that WEPSI can be used for meteorological, agricultural, and hydrological drought monitoring.

Finally, drought events based on WEPSI were compared with El Niño–La Niña years, as well as with El Salvador's annual cereal production. The results indicate that WEPSI is also helpful for agricultural drought assessments because it captures the most critical points of El Salvador's cereal production (i.e., the local maximum and minimum points).

These research outcomes are useful for researchers and policymakers in drought calculation, monitoring, risk assessment, and forecasting. As a future research direction, the application of remote sensing data in calculating WEPSI can be investigated to facilitate the application of WEPSI in other basins. We also suggest testing WEPSI in other case studies and with other purposes. WEPSI's application for drought risk assessment is likewise foreseen.

5 Acknowledgments

Authors thank the grant No. 2579 of the Albert II of Monaco Foundation. VD thanks the Mexican National Council for Science and Technology (CONACYT) and Alianza FiiDEM for the study grand 217776/382365.

6 Author contributions

AK: conceptualization, methodology, investigation, data processing, validation, software, writing—original draft; GACP: conceptualization, project administration, supervision and review; VD: conceptualization, methodology, data processing, writing—review and editing; MA: conceptualization, methodology and review. All authors have read and agreed to the published version of the manuscript.

7 Data Availability statement

All data used for or generated from this study is freely available. WEAP hydrological simulations and the drought indices calculations, incl. WEPSI, are available in Microsoft Excel format. This data is contained in the dataset Lempa River Basin Wet-environment Evapotranspiration and Precipitation Standardized Index (WEPSI), which is available from <http://www.hydroshare.org/resource/b3249a7327ab4bd3a69db091430e1b9d> (Khoshnazar et al., 2021b).

References

- Al Balasmeh, O., Babbar, R., and Karmaker, T. (2020). A hybrid drought index for drought assessment in Wadi Shueib catchment area in Jordan. *Journal of Hydroinformatics*, 22(4), 937-956.
- Aminzadeh, M., and Or, D. (2014). Energy partitioning dynamics of drying terrestrial surfaces. *Journal of Hydrology*, 519, 1257-1270.
- Aminzadeh, M., Roderick, M. L., and Or, D. (2016). A generalized complementary relationship between actual and potential evaporation defined by a reference surface temperature. *Water Resources Research*, 52(1), 385-406.
- Bouchet, R. J. (1963). Evapotranspiration réelle et potentielle, signification climatique. *IAHS Publ*, 62, 134-142.
- Brito, S. S. B., Cunha, A. P. M., Cunningham, C., Alvalá, R. C., Marengo, J. A., and Carvalho, M. A. (2018). Frequency, duration and severity of drought in the Semiarid Northeast Brazil region. *International Journal of Climatology*, 38(2), 517-529.
- Carroll, A. (1998). Natural hazards of North America. Retrieved from <https://catalogue.nla.gov.au/Record/7045960>
- Corzo, P., Diaz, V., and Laverde, M. (2018). Spatiotemporal hydrological analysis. *Int J Hydro*, 2(1), 25-26.
- Corzo Perez, G., Van Huijgevoort, M., Voß, F., and Van Lanen, H. (2011). On the spatio-temporal analysis of hydrological droughts from global hydrological models. *Hydrology and Earth System Sciences*, 15(9), 2963-2978.
- Daryanto, S., Wang, L., and Jacinthe, P.-A. (2017). Global synthesis of drought effects on cereal, legume, tuber and root crops production: A review. *Agricultural Water Management*, 179, 18-33.
- Dash, S. S., Sahoo, B., and Raghuwanshi, N. S. (2021). How reliable are the evapotranspiration estimates by Soil and Water Assessment Tool (SWAT) and Variable Infiltration Capacity (VIC) models for catchment-scale drought assessment and irrigation planning? *Journal of Hydrology*, 592, 125838.
- Dhungel, S., and Barber, M. E. (2018). Estimating calibration variability in evapotranspiration derived from a satellite-based energy balance model. *Remote Sensing*, 10(11), 1695.

- Diaz Mercado, V., Corzo Perez, G., Van Lanen, H. A., and Solomatine, D. (2018). *Comparative analysis of two evaporation-based drought indicators for large-scale drought monitoring*. Paper presented at the EGU General Assembly Conference Abstracts.
- Diaz, V., Perez, G. A. C., Van Lanen, H. A., Solomatine, D., and Varouchakis, E. A. (2020). An approach to characterise spatio-temporal drought dynamics. *Advances in Water Resources*, 137, 103512.
- Encyclopedia of the Nations. (2021). *El Salvador - Agriculture*. Retrieved from <https://www.nationsencyclopedia.com/economies/Americas/El-Salvador-AGRICULTURE.html>
- Food and Agriculture Organization (FAO) of the United Nations (UN). (2021). *GIEWS - Global Information and Early Warning System. Country Briefs. El Salvador*. Retrieved from <http://www.fao.org/giews/countrybrief/country.jsp?code=SLV&lang=en>
- Fisher, J. B., Whittaker, R. J., and Malhi, Y. (2011). ET come home: potential evapotranspiration in geographical ecology. *Global Ecology and Biogeography*, 20(1), 1-18.
- Freshplaza. (2021). *Agricultural industry in El Salvador reports heavy losses due to rainfall*. Retrieved from <https://www.freshplaza.com/article/9267702/agricultural-industry-in-el-salvador-reports-heavy-losses-due-to-rainfall/>
- Global Environment Facility. (2019). *Fostering Water Security in the Trifinio Region: Promoting the formulation of a TDA/SAP for its transboundary Lempa River Basin*. Retrieved from <https://www.thegef.org/project/fostering-water-security-trifinio-region-promoting-formulation-tdasap-its-transboundary>
- Granger, R. (1989). A complementary relationship approach for evaporation from nonsaturated surfaces. *Journal of Hydrology*, 111(1-4), 31-38.
- Han, S., and Tian, F. (2020). A review of the complementary principle of evaporation: from the original linear relationship to generalized nonlinear functions. *Hydrology and Earth System Sciences*, 24(5), 2269-2285.
- Helman, P., and Tomlinson, R. (2018). Two centuries of climate change and climate variability, East Coast Australia. *Journal of Marine Science Engineering*, 6(1), 3.
- Hernández, W. (2005). Nacimiento y Desarrollo del río Lempa. *MARN/SNET*.
- Homdee, T., Pongput, K., and Kanae, S. (2016). A comparative performance analysis of three standardized climatic drought indices in the Chi River basin, Thailand. *Agriculture and Natural Resources*, 50(3), 211-219.
- Jennewein, J. S., and Jones, K. W. (2016). Examining ‘willingness to participate’ in community-based water resource management in a transboundary conservation area in Central America. *Water Policy*, 18(6), 1334-1352.
- Kahler, D. M., and Brutsaert, W. (2006). Complementary relationship between daily evaporation in the environment and pan evaporation. *Water Resources Research*, 42(5).
- Karim, M. R., and Rahman, M. A. (2015). Drought risk management for increased cereal production in Asian least developed countries. *Weather and Climate Extremes*, 7, 24-35.
- Khoshnazar, A., Corzo Perez, G. A., and Diaz, V. (2021a). Spatiotemporal Drought Risk Assessment Considering Resilience and Heterogeneous Vulnerability Factors: Lempa Transboundary River Basin in The Central American Dry Corridor. *Journal of Marine Science and Engineering*, 9(4), 386.

- Khoshnazar, A., Corzo Perez, G. A., Diaz, V., and Aminzadeh, M. (2021b). Lempa River Basin Wet-environment Evapotranspiration and Precipitation Standardized Index (WEPSI) Data. *HydroShare*, <http://www.hydroshare.org/resource/b3249a7327ab4bd3a69db091430e1b9d>
- Kim, D., and Rhee, J. (2016). A drought index based on actual evapotranspiration from the Bouchet hypothesis. *Geophysical Research Letters*, 43(19), 10,277-210,285.
- Kim, J. S., Jain, S., Lee, J. H., Chen, H., and Park, S. Y. (2019). Quantitative vulnerability assessment of water quality to extreme drought in a changing climate. *Ecological Indicators*, 103, 688-697.
- Koppa, A., Alam, S., Miralles, D. G., and Gebremichael, M. (2021). Budyko-Based Long-Term Water and Energy Balance Closure in Global Watersheds From Earth Observations. *Water Resources Research*, 57(5), e2020WR028658.
- Kumar, P., Masago, Y., Mishra, B. K., and Fukushima, K. (2018). Evaluating future stress due to combined effect of climate change and rapid urbanization for Pasig-Marikina River, Manila. *Groundwater for Sustainable Development*, 6, 227-234.
- Lewis, J., Rowland, J., and Nadeau, A. (1998). Estimating maize production in Kenya using NDVI: some statistical considerations. *International Journal of Remote Sensing*, 19(13), 2609-2617.
- Lu, Z., Zhao, Y., Wei, Y., Feng, Q., and Xie, J. (2019). Differences among evapotranspiration products affect water resources and ecosystem management in an Australian catchment. *Remote Sensing*, 11(8), 958.
- El Salvador's Ministry of Environment and Natural Resources (MARN). (2019a). *Ministerio de Medio Ambiente y Recursos Naturales*. San Salvador, El Salvador. Retrieved from <https://www.marn.gob.sv/>
- El Salvador's Ministry of Environment and Natural Resources (MARN). (2019b). *Water Resources Maps*. San Salvador, El Salvador. Retrieved from https://web.archive.org/web/20090422151648/http://snet.gob.sv/cd2/SeccionSIG/map_hi.htm
- McKee, T. B., Doesken, N. J., and Kleist, J. (1993). *The relationship of drought frequency and duration to time scales*. Paper presented at the Proceedings of the 8th Conference on Applied Climatology.
- Mera, Y. E. Z., Vera, J. F. R., and Pérez-Martín, M. Á. (2018). Linking El Niño Southern Oscillation for early drought detection in tropical climates: The Ecuadorian coast. *Science of The Total Environment*, 643, 193-207.
- Mukherjee, S., Mishra, A., and Trenberth, K. E. (2018). Climate change and drought: a perspective on drought indices. *Current Climate Change Reports*, 4(2), 145-163.
- National Oceanic and Atmospheric Administration. (2015). *The El Niño Southern Oscillation (ENSO) is one of the most important climatic phenomena on Earth*. Retrieved from <https://www.noaa.gov/education/resource-collections/weather-atmosphere/el-nino>
- Nkemdirim, L., and Weber, L. (1999). Comparison between the droughts of the 1930s and the 1980s in the southern prairies of Canada. *Journal of Climate*, 12(8), 2434-2450.
- Oti, J. O., Kabo-Bah, A. T., and Ofosu, E. (2020). Hydrologic response to climate change in the Densu River Basin in Ghana. *Heliyon*, 6(8), e04722.
- Palmer, W. C. (1965). *Meteorological drought* (Vol. 30): US Department of Commerce, Weather Bureau.

- Palmer, W. C. (1968). Keeping track of crop moisture conditions, nationwide: the new crop moisture index.
- Peters, E., Torfs, P., Van Lanen, H. A., and Bier, G. (2003). Propagation of drought through groundwater—a new approach using linear reservoir theory. *Hydrological processes*, 17(15), 3023-3040.
- Priestley, C. H. B., and Taylor, R. J. (1972). On the assessment of surface heat flux and evaporation using large-scale parameters. *Monthly weather review*, 100(2), 81-92.
- Seiber, J., and Purkey, D. (2015). WEAP—Water Evaluation and Planning System User Guide for WEAP 2015. *Stockholm Environment Institute*.
- Sheffield, J., Goteti, G., and Wood, E. F. (2006). Development of a 50-year high-resolution global dataset of meteorological forcings for land surface modeling. *Journal of Climate*, 19(13), 3088-3111.
- Shukla, S., and Wood, A. W. (2008). Use of a standardized runoff index for characterizing hydrologic drought. *Geophysical Research Letters*, 35(2).
- Sorí, R., Vázquez, M., Stojanovic, M., Nieto, R., Liberato, M. L., Gimeno, L. J. N. H., and Sciences, E. S. (2020). Hydrometeorological droughts in the Miño–Limia–Sil hydrographic demarcation (northwestern Iberian Peninsula): the role of atmospheric drivers. 20(6), 1805-1832.
- Speich, M. J. (2019). Quantifying and modeling water availability in temperate forests: a review of drought and aridity indices. *iForest-Biogeosciences and Forestry*, 12(1), 1.
- The World Bank Group. (2021). *Cereal production (metric tons) - El Salvador*. Retrieved from <https://data.worldbank.org/indicator/AG.PRD.CREL.MT?locations=SV>
- Vergara, J. R., and Estévez, P. A. (2014). A review of feature selection methods based on mutual information. *Neural computing and applications*, 24(1), 175-186.
- Vicente-Serrano, S. M. (2006). Differences in spatial patterns of drought on different time scales: an analysis of the Iberian Peninsula. *Water resources management*, 20(1), 37-60.
- Vicente-Serrano, S. M., Beguería, S., and López-Moreno, J. I. (2010). A multiscalar drought index sensitive to global warming: the standardized precipitation evapotranspiration index. *Journal of Climate*, 23(7), 1696-1718.
- Vicente-Serrano, S. M., Miralles, D. G., Domínguez-Castro, F., Azorin-Molina, C., El Kenawy, A., McVicar, T. R., . . . Peña-Gallardo, M. (2018). Global assessment of the Standardized Evapotranspiration Deficit Index (SEDI) for drought analysis and monitoring. *Journal of Climate*, 31(14), 5371-5393.
- Wang, D., Hejazi, M., Cai, X., and Valocchi, A. J. (2011). Climate change impact on meteorological, agricultural, and hydrological drought in central Illinois. *Water Resources Research*, 47(9).
- Wang, Y., Yang, J., Chen, Y., Su, Z., Li, B., Guo, H., and De Maeyer, P. (2020). Monitoring and Predicting Drought Based on Multiple Indicators in an Arid Area, China. *Remote Sensing*, 12(14), 2298.
- Wells, N., Goddard, S., and Hayes, M. J. (2004). A self-calibrating Palmer drought severity index. *Journal of Climate*, 17(12), 2335-2351.
- Wen, W., Timmermans, J., Chen, Q., and van Bodegom, P. M. (2021). A Review of Remote Sensing Challenges for Food Security with Respect to Salinity and Drought Threats. *Remote Sensing*, 13(1), 6.
- Wilhite, D. A., and Glantz, M. H. (1985). Understanding: the drought phenomenon: the role of definitions. *Water international*, 10(3), 111-120.

- 784 Xiao, M., Yu, Z., Kong, D., Gu, X., Mammarella, I., Montagnani, L., . . . Lohila, A. (2020).
785 Stomatal response to decreased relative humidity constrains the acceleration of terrestrial
786 evapotranspiration. *Environmental Research Letters*, 15(9), 094066.
- 787 Yihdego, Y., Vaheddoost, B., and Al-Weshah, R. A. (2019). Drought indices and indicators
788 revisited. *Arabian Journal of Geosciences*, 12(3), 69.
- 789 Zargar, A., Sadiq, R., Naser, B., and Khan, F. I. (2011). A review of drought indices.
790 *Environmental Reviews*, 19(NA), 333-349.
- 791 Zhang, J., Bai, Y., Yan, H., Guo, H., Yang, S., and Wang, J. (2020). Linking observation,
792 modelling and satellite-based estimation of global land evapotranspiration. *Big Earth*
793 *Data*, 4(2), 94-127.
- 794 Zheng, C., Jia, L., Hu, G., and Lu, J. (2019). Earth Observations-Based Evapotranspiration in
795 Northeastern Thailand. *Remote Sensing*, 11(2), 138.

796